JOURNAL OF OPTOELECTRONICS AND ADVANCED MATERIALS Vol. 9, No. 1, January 2007, p. 92 - 98

Invited Lecture

Deposition processes for high efficiency microcrystalline silicon solar cells

F. FINGER[a*], R. CARIUS[a], X. GENG[b], S. KLEIN[a,c], Y. MAI[a.b,d], M. SENDOVA-VASSILEVA[e]
[a]*Forschungszentrum Jülich, Institut für Photovoltaik, 52425 Jülich, Germany*
[b] *Nankai University, Institute of Photoelectronics, Weijin Road 94, Tianjin 300071, PR China*
[c]*now at: Applied Materials GmbH & Co. KG, Siemensstr. 100, 63755 Alzenau, Germany*
[d]*now at: Utrecht University, Faculty of Science, P.O. Box 80000, 3508 TA Utrecht, The Netherlands*
[e]*Central Laboratory for Solar Energy and New Energy Sources, Bulgarian Academy of Sciences, 72 Tzarigradsko Chaussee Blvd., 1784 Sofia, Bulgaria*

Examples of recent achievements in the preparation of microcrystalline silicon for solar cell application are shown. The requirements on the deposition process given by the needs to prepare material with an optimum phase mixture are demonstrated. A focus is on the VHF-PECVD technique in the high-power, high-pressure regime. The advantage of the HWCVD process for improved interface performance is shown. Introduction of a buffer layer allows one to apply a high deposition rate processes and to achieve record solar cell efficiencies of 10.3% for a single junction µc-Si:H pin.

(Received November 1, 2006; accepted December 21, 2006)

Keywords: Microcrystalline silicon, Thin film solar cells, PECVD, HWCVD

1. Introduction

The preparation of microcrystalline silicon (µc-Si:H) has made considerable progress over the last ten years, in terms of deposition rates (R_D) and material quality for solar cell applications. A breakthrough was the use of higher plasma excitation frequencies in plasma enhanced chemical vapour deposition (PECVD) in place of the standard 13.56 MHz [1-3]. A further important technological development was made when turning back to the 13.56 MHz excitation by use of the high-pressure, high-power (hphP) method [4-6] and lately by combination of high excitation frequencies (VHF) with hphP [5, 7-12]. On the other hand, record conversion efficiencies were also obtained with µc-Si:H absorber layers prepared with hot wire (HW) CVD [13]. While similar high efficiencies are obtained with the two processes, PECVD and HWCVD, there are also distinct differences in the performance of the resulting solar cells [12, 13]. Recently, using a combination of the two deposition processes, single junction µc-Si:H solar cells with efficiencies above 10% have been reported, where the bulk of the i-layer was deposited at 1.1 nm/s [14, 15]. In the present report, we will review some of the recent results obtained for µc-Si:H films and solar cells prepared by PECVD and HWCVD. We will start with a brief overview of important µc-Si:H material properties relevant for solar cell performance, in particular related to instability in the material. The observed effects related to the structure of the material put certain constrains on the preparation process. For instance it has been shown that high temperatures and high deposition rate processes in general lead to inferior material properties like a pronounced porosity, low hydrogen content and high defect density. For PECVD, a high discharge power may lead to high ion energy bombardment of the growing material. For HWCVD, high deposition rate processes go hand in hand with high filament temperatures and high thermal load on the substrate. A further optimization of µc-Si:H deposition processes at high growth rates and homogeneously on large areas is needed, and will be a major R&D effort in the next few years as the a-Si:H/µc-Si:H solar cell technology enters into multi-megawatt production.

2. Experiment

Microcrystalline silicon material is prepared with PECVD at excitation frequencies in the VHF

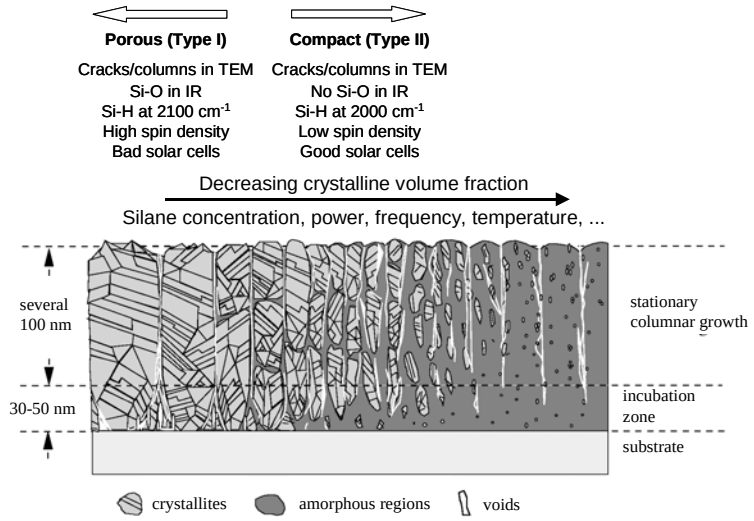

Fig. 1. Schematic diagram showing microstructure features of µc-Si:H. From left to right the film composition changes from highly crystalline to predominantly amorphous.

band (95 MHz) [12] or with HWCVD using tantalum wires [13]. The preparation of individual layers and solar cells is done in a cluster tool deposition system with one chamber dedicated to the PECVD and HWCVD process respectively, and two other chambers for p- and n-layers, both with PECVD. This arrangement allows direct comparison of the solar cells with either PECVD layer or HWCVD layer while keeping the doped layers the same. In addition, the versatile reactor geometry allows easy adjustment of e.g. the electrode or wire distance to the substrate, variation of excitation frequency or wire material, application of a shutter during process start, etc. Finally it allows the combination of layers of PECVD and HWCVD in a favourable way, as we shall demonstrate. Solar cells were deposited in *p-i-n* sequence on 10×10cm² texture-etched ZnO-coated glass substrates. The 1×1cm² back contact (Ag or highly reflective ZnO/Ag for selected samples) defines the individual solar cell area. The microcrystalline *p*-layer and amorphous *n*-layer were prepared by PECVD. The *i*-layers of HWCVD solar cells and the high quality HW buffer layers were deposited using Ta filaments. For PECVD of the µc-Si:H absorber layers, we explore the high pressure high power (hphP) regime and shall show results upon variation of the silane concentration, $SC = [SiH_4] / ([SiH_4] + [H_2])$, the discharge power ($P_{VHF}$) and pressure ($p_D$), and the total gas flow (Fl_{total}). The Raman intensity ratio I_C^{RS} [16] is used as a semi-quantitative value for the crystalline volume fraction. Further details of the material and solar cell preparation are published elsewhere [12, 13].

3. Results

Fig 1 shows a diagram of the µc-Si:H structure from highly crystalline (left) to amorphous (right) [17]. A key feature of the material, typically found on the crystalline side, is the pronounced porosity accompanied by a high surface sensitivity to contamination – concluded from the strong Si-O absorption modes in the infrared spectra -, a high defect density and low device performance. Also the dominance of the Si-H absorption mode at 2100 cm^{-1} over the one at 2000 cm^{-1} indicates the presence of internal surfaces. More compact structures are found usually in the transition between crystalline and amorphous growth, a material which may contain a considerable fraction of the amorphous phase. Such material has low spin densities, a predominant Si-H absorption at 2000 cm^{-1} indicating hydrogen in a compact, bulk phase, and yields high efficiency solar cells [12, 13, 17]. Such material shows no Si-O absorption in the infrared spectra, even though also in this material deep cracks and columns are observed in the TEM images. We shall distinguish the material into Type I and Type II [18].

An interesting consequence of using material with a mixed structure for high efficiency solar cells is the occurrence of light induced degradation in Type II material (Fig. 2) [19].

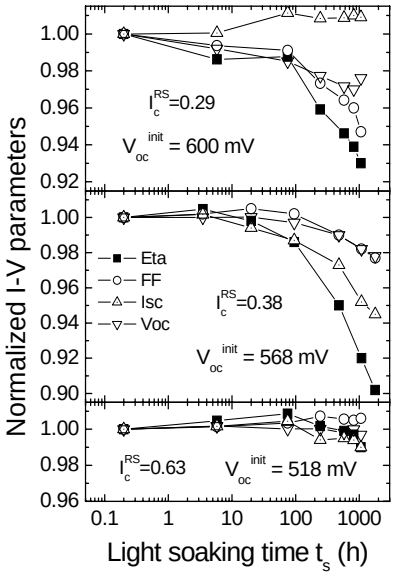

Fig. 2. Dependence of µc-Si:H solar cell parameters as a function of light soaking time. From top to bottom the material has increasing crystalline volume fractions which results typically in lower V_{OC} values.

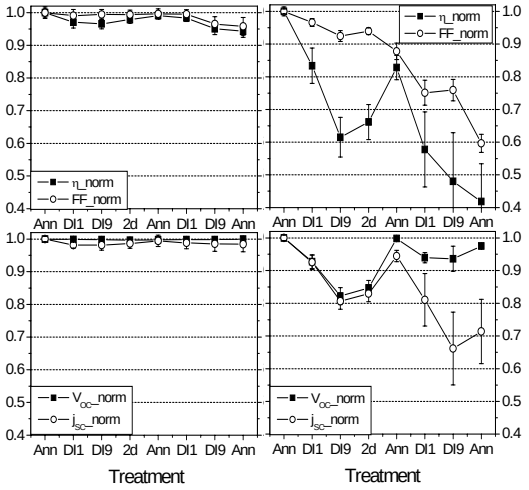

Fig. 3. Normalized J-V parameters under AM 1.5 of solar cells with i-layer deposited by HWCVD after different treatments: Ann – annealing at 160 °C in air, DIn – n hours in de-ionized water, 2d – 2 days in ambient conditions: Type I (right), Type II (left) .

The figure shows the light soaking behaviour of solar cells prepared by HWCVD with i-layers of different crystal volume fraction. Presumably compact, Type II material with I_C^{RS} = 0.29 & 0.38 shows an efficiency degradation of up to 10% after 1000h illumination. Note that this material results in high open circuit voltages and efficiencies comparing materials with different I_C^{RS} values. Material with a high crystal volume fraction (possibly porous, Type I material) instead is completely stable upon light soaking (lower curve in Fig. 2).

However, when looking for stability against exposure to air or water, it is the Type I material which shows degradation. In Fig. 3 the behaviour of solar cells with compact or porous absorber layer material upon treatment in water and after annealing is compared. While compact material shows no degradation, the solar cells with highly crystalline material result in a non-reversible degradation after treatment in water [20].

Any development of the deposition process will have to consider these effects, finding an optimum compromise. In most circumstances, variation of the material structure to cover the range from crystalline to amorphous in order to find optimum phase mixture (OPM) material seems mandatory.

Such an optimization process is demonstrated here for the development of the high pressure, high power growth regime with VHF-PECVD. The hphP deposition was suggested to provide effective gas decomposition for high deposition rates and microcrystalline growth while keeping ion energies low [4, 5]. Combination of hphP with the inherently low ion energy process VHF-PECVD promises additional advantages.

Fig. 4 shows the deposition rate vs. SC for variation of the discharge power, pressure and electrode distance. R_D increases linearly with SC, but shows little influence of the RF power, which suggests partial depletion of the silane.

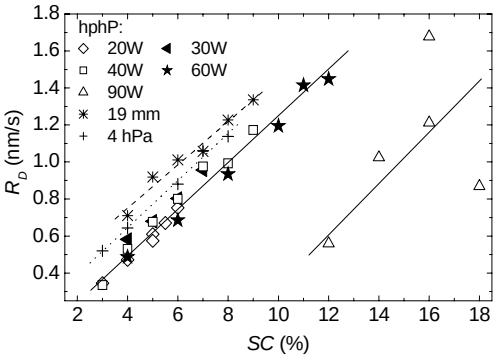

Fig. 4. R_D of solar cells deposited with PECVD at different P_{VHF} vs. SC. p_{depo} = 2.1 hPa and d = 12 mm were used for most of the series, except for the two series with higher p_{depo} (hphP 4 hPa) or larger electrode distance (hphP 19 mm).

This is supported by the observation of a higher deposition rate when increasing the pressure from 2.1 to 4 hPa or the electrode distance from 12 to 19 mm. In both cases, more silane is available in the plasma reaction zone. At 90W input power, a strongly in-homogeneous deposition is observed, showing the upper limit of the present reactor geometry concerning maximum discharge power.

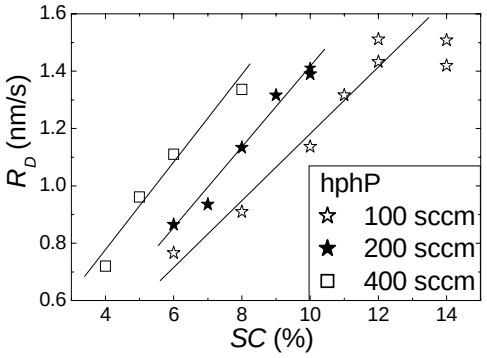

Fig. 5. R_D of solar cells deposited with PECVD at different Fl_{total}, a power of 60 W, pressure of 2.1 hPa, and electrode distance of 12 mm.

Also, when increasing the total gas flow Fl_{total}, i.e. both the silane and the hydrogen flow by the same factor, the deposition rate increases at a given SC when keeping all other deposition parameters constant (Fig. 5). At higher Fl_{total}, more silane is available in the reaction zone, counteracting depletion.

The transition from highly crystalline to amorphous growth is not evident from any features in the R_D vs. *SC* curve in Figs. 4&5, but a structural transition can be concluded from the solar cell performance (Fig. 6&7). Fig 6 summarizes the effects of different discharge powers on the solar cell performance. We see the typical behaviour of the current-voltage characteristics as the material changes from highly crystalline to amorphous [12, 13, 17]. The transition from crystalline to amorphous growth is

identified with the drop in *FF* and J_{SC} at a certain SC. The transition shifts to higher *SC* as the power increases. As the deposition rate increases with SC, such a shift means that the highest efficiency solar cells are prepared at higher deposition rates, as one increases the discharge power (compare with Fig. 4). With an increase in the total gas flow, the transition from crystalline to amorphous growth shifts to lower *SC*, as can be concluded from the *J-V* parameters of these cells (Fig. 7). Again, similar dependencies of the solar cell parameters are observed with variation of *SC* for all different Fl_{total} and the transition is identified with the drop in *FF* and J_{SC}. As the optimum solar cells are prepared at lower *SC* when increasing Fl_{total}, the corresponding deposition rates decrease slightly (compare with Fig. 5). Note: The solar cells with variations of total gas flow (Fig. 7) were prepared at a later stage with optimized, thinner p-layers as compared with the hphP 60 W series in Fig. 6. This results in an increase of the blue light response and thus J_{SC}, leading to higher efficiencies.

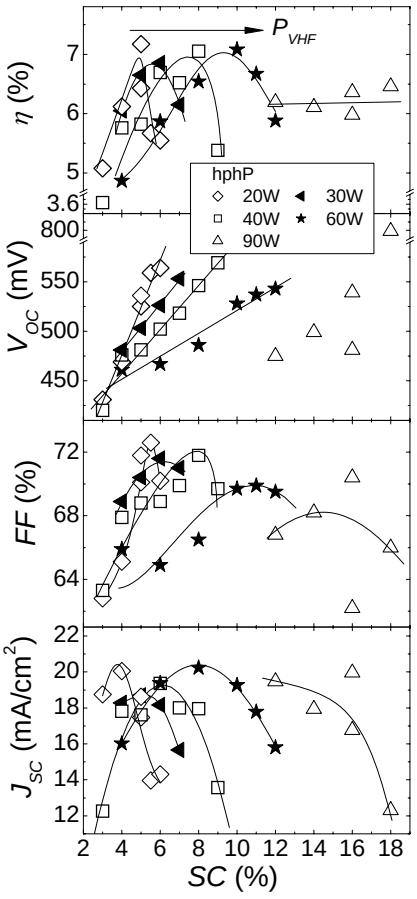

Fig. 6. J-V parameters of solar cells deposited under hphP conditions with different P_{VHF}. Solar cells are ~1 μm thick and have an area of 1×1 cm², defined by Ag back contacts. The arrow in the upper figure shows the shift of the optimum cells' SC upon the increasing P_{VHF} .

Direct evidence for the shift in the transition from a crystalline to an amorphous structure comes from Raman scattering experiments of the i-layer material. Fig. 8 summarizes I_c^{RS} data obtained for a number of samples from Figs. 6&7, i.e. prepared with different power and total gas flow as a function of silane concentration.

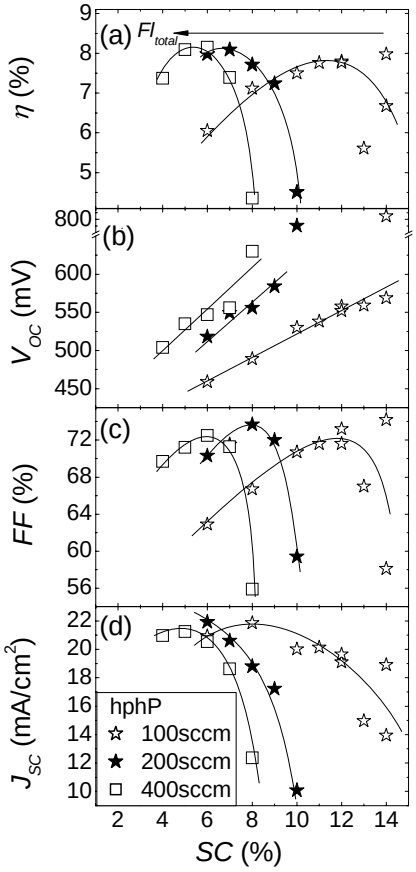

Fig. 7. J-V- parameters of solar cells deposited with different Fl_{total}. The arrow in figure (a) shows the systematic shift of the optimum cells' SC upon the increasing Fl_{total}.

The shift in the structure transition with variation in P_{VHF} and Fl_{total} is indicated. We find that the best solar cell performance is always obtained for an I_c^{RS} value of about 0.6, which we call the optimum phase mixture (OPM).

Most importantly, however, it was found that the quality of the μc-Si:H solar cells can be maintained at a high level independent of the deposition rate R_D. In Fig. 9, the *FF* and V_{OC} of the optimum cells of the individual series are plotted versus the deposition rate. Both quantities as a measure of the absorber layer quality maintain a high level, independent from the deposition rate. The highest efficiencies for single junction μc-Si:H pin solar cells are 9.8% at an i-layer deposition rate of 1.1 nm/s [12].

With HWCVD [21], such a combination of high R_D and high efficiency has not been obtained so far. High R_D of μc-Si:H obtained with effective gas decomposition at high filament temperatures are at the cost of the material quality [13].

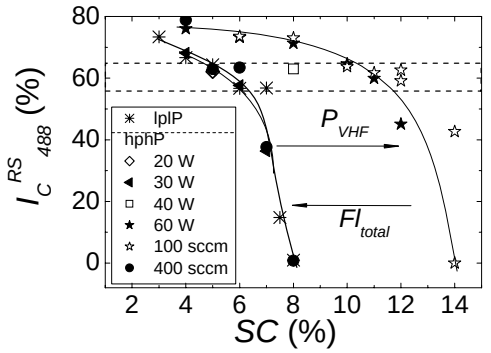

Fig. 8. Raman scattering intensity ratio, I_C^{RS}, of µc-Si:H solar cells. The best cells in the SC series are found between the two dashed lines. Arrows in the figure indicate the shift of I_C^{RS} by applying higher P_{VHF} or Fl_{total}.

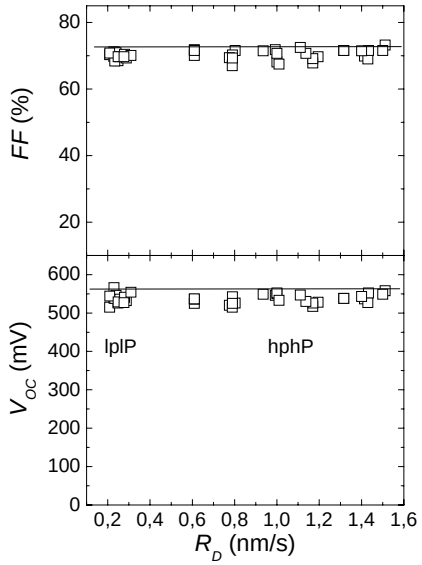

Fig. 9. FF and V_{OC} of the optimum µc-Si:H solar cells deposited under lplP and hphP conditions vs. R_D. Samples with R_D above 0.6 nm/s are deposited with hphP and those below 0.35 nm/s with lplP. Lines in the figure are guides to the eye as the upper limit of the two J-V parameters.

The heat transfer from the filament to the substrate, resulting in too high deposition temperatures, is seen as an obstacle here. Attempts have been made to increase the deposition rate in the HWCVD process: keeping the substrate temperature low by reduction of the filament temperature, increasing the filament-to-substrate distance, using different wire geometries or a higher deposition pressure [22]. In Fig. 10, the deposition rate and the microstructure factor (the ratio of the Si-H infrared absorption modes as a measure of porosity [22]) is shown for material grown with HWCVD with a variety of filament configurations and settings in such a way that the substrate temperature was kept at 250°C. In the region of interest for µc-Si:H solar cell application of I_c^{RS} = 40…60%, the deposition rate can be increased to some extent. Still the increase in deposition rate is generally accompanied by lower material quality, as seen in the microstructure factor. Nevertheless, when keeping the substrate temperature at around 200 °C with deposition rates of 0.1 nm/s, µc-Si:H solar cell efficiencies well above 9% were achieved with the HWCVD process (Fig. 11) [13]. In addition, the HWCVD process appears to have some advantages for high quality µc-Si:H material and device deposition. The cells with material prepared with HWCVD at a given material composition show considerably higher open circuit voltages V_{OC} than those prepared with PECVD (Fig. 9) [13-15].

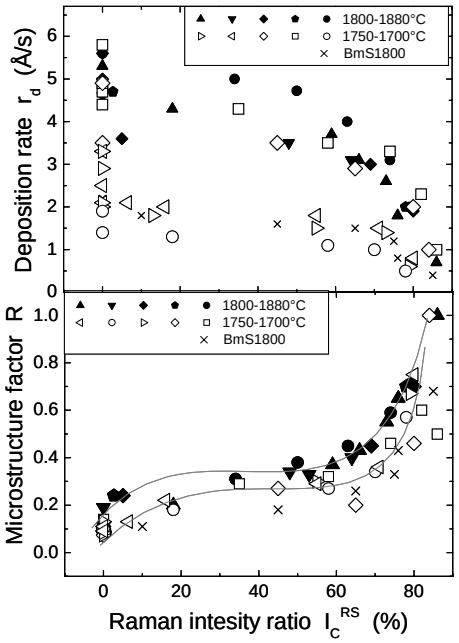

Fig. 10. Deposition rate (top) and microstructure factor (bottom) for Si thin films prepared with HWCVD vs. I_c^{RS} for various filament configurationsn all resulting in a substrate temperature of 250°C.

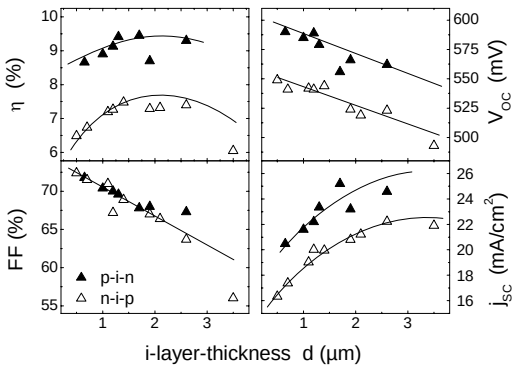

Fig. 11. J-V parameters of µc-Si:H solar cells prepared with HWCVD at a low substrate temperature in pin (T_S=185 °C) or nip (T_S = 260 °C) configurations with different i-layer thickness.

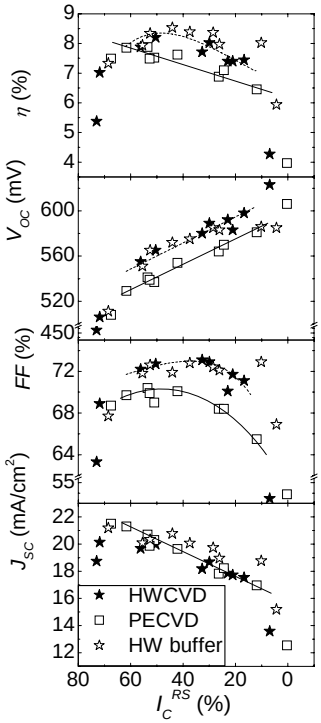

Fig. 12. J-V parameters of µc-Si:H solar cells with i layers deposited by (i)PECVD, (ii) HWCVD or (iii) by PECVD with a 100 nm HWCVD buffer at the p/i interface vs. I_c^{RS}.

We have identified the p/i interface region as the main source for a slightly inferior performance of the PECVD material with respect to V_{OC} and spectral blue response [14, 15]. By introduction of an intrinsic buffer layer prepared by HWCVD directly on the p-layer, these differences are completely removed (Fig. 9). We thus are able to combine high V_{OC} material with a high deposition rate processes. Fig. 13 shows the I-V curves of such solar cells with 10.3% efficiency, where the bulk i-layer was prepared at 1.1 nm/s.

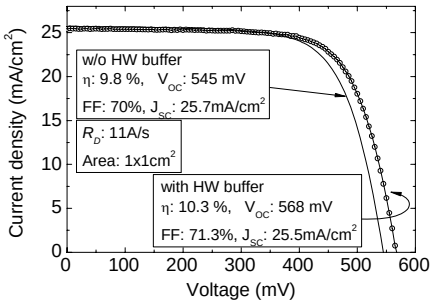

Fig. 13. A HW p/i buffer layer improves the V_{OC} and FF of a µc-Si:H single junction solar cell resulting in a high efficiency of 10.3% with the bulk i-layer deposited at a R_D of 1.1 nm/s.

4. Discussion

4.1. VHF-PECVD

The observations during development of the growth process for µc-Si:H with VHF-PECVD under hphP conditions are explained in a schematic picture which considers maintenance of the appropriate ratio of H over SiH_x radicals a key issue to obtain OPM µc-Si:H material growth [12].

We propose that a proper ratio of atomic H over SiH_x (x= 1, 2 or 3) should be maintained for the OPM material growth. Note that the contribution to the growth from individual kinds of radical, such as SiH, SiH_2 or SiH_3, will not be elaborated on in this paper. Let us first look at the influence of P_{VHF}, which is visualized in the schematic diagram in Fig. 14 (a). At low P_{VHF}, a certain H/SiH_x ratio for the OPM material growth is established by the choice of *SC*. A higher P_{VHF} cannot produce more silicon-related precursors, due to the silane depletion in the whole investigated *SC* range. But it will increase the atomic H density further, resulting in a higher H/SiH_x ratio. This effect does not lead to higher R_D, but higher crystallinity in the *i* layer (confirmed by the results of Figs. 6 & 8). In order to compensate the increased hydrogen radical density and maintain the required H/SiH_x ratio for the OPM material growth, more silane has to be added to the plasma, leading to higher R_D for the optimum solar cell.

Fig. 14 (b) illustrates the situation for different Fl_{total}, which fits well into this picture, too. When a higher Fl_{total} is applied to an established OPM material growth condition, higher R_D will be generally observed because of the higher silane supply (see Fig. 5). But the increasing number of SiH_x radicals and the possible atomic H annihilation effect by the excessive silane molecules results in a lower H/SiH_x ratio, leading to lower *i* layer crystallinity. This is confirmed by the Raman scattering measurements (Fig. 8) and by the *J-V* parameters (Fig. 7) of the solar cells deposited with different Fl_{total}. In order to maintain the proper ratio of atomic H over SiH_x, one has to go to lower *SC* at higher $Fl_{total.}$

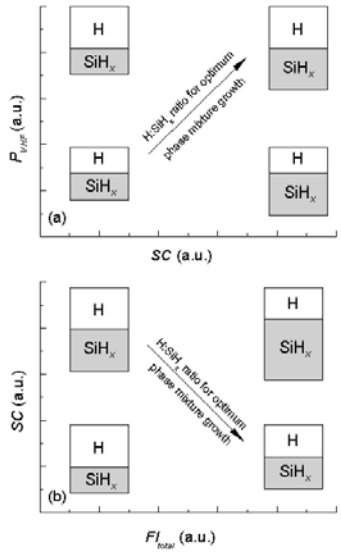

Fig. 14. Schematic diagram of the amount of hydrogen and silane radicals (arbitrary units) under hphP conditions in the (a) "SC – P_{VHF}" and (b) "Fl_{total} – SC" parameter space. To maintain the proper H/SiH_x ratio for growth of optimum phase mixture material, the SC has to be adjusted when varying P_{VHF} or Fl_{total}.

Under a high Fl_{total} condition, the optimum solar cells are prepared at lower R_D than those at low Fl_{total}, although the total silane flow rate for the optimum cell is still higher. This is an indication of lower gas utilization under high Fl_{total} conditions, resulting from a shorter gas residence time.

As the variation of *SC* is the most simple and straightforward method to adjust the H/SiH_x ratio, we consider it mandatory for material and device optimization.

4.2. HWCVD

The HWCVD process, when restricted to low substrate temperatures, gives favorable conditions for high quality µc-Si:H growth and control of interface properties, resulting in solar cells with high open circuit voltages and fill factors. A possible reason is the absence of ion bombardment in the hot wire process.

Achieving high deposition rates with HWCVD for µc-Si:H with high quality will be a challenge. Adjustments to the filament geometry or active substrate cooling are possible solutions.

4. Conclusions

VHF-PECVD at high pressure and high power (hphP) was developed successfully for deposition of µc-Si:H solar cells at high rates.

In this regime the deposition rate can be varied considerably, without influence on the high quality solar cell performance.

To determine the conditions to obtain optimum phase mixture (OPM) material, variation of the deposition parameters to cover the crystalline-to-amorphous transition is required.

The benefits of the HWCVD process to result in higher V_{OC} are combined with high deposition rate processes. By introduction of a HW buffer layer, an efficiency of 10.3% is obtained for a single junction µc-Si:H pin cell.

Acknowledgements

We thank F. Birmanns, M. Hülsbeck, A. Lambertz, S. Michel, W. Reetz, G. Schöpe, H. Siekmann, H. Stiebig, J. Wolff, Ch. Zahren and B. Zwaygardt for important contributions to this work.

References

[1] S. Oda, J. Noda, M. Matsumura, Mat. Res. Soc. Symp. Proc. **118,** 117 (1988).
[2] K. Prasad, F. Finger, H. Curtins, A. Shah, J. Baumann, Mat. Res. Soc. Symp. Proc. **164,** 27 (1990).
[3] F. Finger, P. Hapke, M. Luysberg, R. Carius, H. Wagner, M. Scheib, Appl. Phys. Lett. **65,** 2588 (1994).
[4] L. Guo, M. Kondo, M. Fukawa, K. Saitoh, A. Matsuda, Jpn. J. Appl. Phys. **37**, L1116 (1998).
[5] M. Kondo, M. Fukawa, L. Guo, A. Matsuda, J. Non-Cryst. Solids **266-269,** 84-89 (2000).
[6] T. Roschek, T. Repmann, J. Müller, B. Rech, H. Wagner, J. Vac. Sci. Technol. A **20**, 492 (2002).
[7] M. Fukawa, S. Suzuki, L. Guo, M. Kondo, A. Matsuda, Sol. Energ. Mat. Sol. C. **66**, 217 (2001).
[8] T. Matsui, M. Tsukiji, H. Saika, T. Toyama, H. Okamoto, Jpn. J. Appl. Phys. **41**, 20 (2002).
[9] U. Graf, J. Meier, U. Kroll, J. Bailat, C. Droz, E. Vallat-Sauvain, A. Shah, Thin Solid Films **427**, 37 (2003).
[10] Lambertz, O. Vetterl, F. Finger, Proc. 17th EPVSEC, ed. B. McNelis, W. Palz, H.A. Ossenbrink and P. Helm (WIP-Renewable Energies, Munich) 2977 (2001).
[11] J. K. Rath, R. H. J. Franken, A. Gordijn, R. E. I. Schropp, W. J. Goedheer, J. Non-Cryst. Solids **338-340**, 56 (2004).
[12] Y. Mai, S. Klein, R. Carius, J. Wolff, A. Lambertz, F. Finger, X. Geng, J. Appl. Phys. **97**, 114913 (2005).
[13] S. Klein, F. Finger, R. Carius, M. Stutzmann, J. Appl. Phys. **98**, 024905 (2005).
[14] Y. Mai, S. Klein, R. Carius, H. Stiebig, X. Geng, F. Finger, Appl. Phys. Lett. **87**, 073503 (2005)
[15] S. Klein, Y. Mai, F. Finger, M. V. D. Donker, R. Carius, H. Stiebig, Proc. 15th International Photovoltaic Science & Engineering Conference, Shanghai, China, pp. 736 (2005)
[16] L. Houben, M. Luysberg, P. Hapke, R. Carius, F. Finger, H. Wagner, Philos. Mag. A **77,** 1447 (1998).
[17] Vetterl, F. Finger, R. Carius, P. Hapke, L. Houben, O. Kluth, A. Lambertz, A. Mück, B. Rech, H. Wagner, Sol. Energ. Mat. Sol. C. **62,** 97 (2000).
[18] F. Finger, R. Carius, T. Dylla, S. Klein, S. Okur, M. Günes, IEE Proceedings - Circuits, Devices and Systems **150**, 300 (2003).
[19] S. Klein, F. Finger, R. Carius, T. Dylla, B. Rech, M. Grimm, L. Houben, M. Stutzmann, Thin Solid Films **430**, 202 (2003).
[20] M. Sendova-Vassileva, F. Finger, S. Klein, A. Lambertz, J. Optoelectron. Adv. Mater **7**, 481 (2005).
[21] H. Matsumura, Jpn. J. Appl. Phys. Part 1 **37**, 3175 (1998).
[22] S. Klein, F. Finger, R. Carius, J. Lossen, Thin Solid Films **501,** 43 (2006).

*Corresponding author: f.finger@fz-juelich.de